Growth of nanodroplets on a still microfiber under flow conditions

Journal:	*Physical Chemistry Chemical Physics*
Manuscript ID	CP-ART-04-2018-002353.R1
Article Type:	Paper
Date Submitted by the Author:	08-Jun-2018
Complete List of Authors:	Yu, Haitao; RMIT University, School of Engineering Rump, Maaike; Universiteit Twente Maheshwari, Shantanu; University of Twente, Science and Engineering Bao, Lei; RMIT University, School of Civil, Environmental and Chemical Engineering Zhang, Xuehua; University of Alberta, Chemical & Materials Engineering; University of Alberta,

PCCP

ROYAL SOCIETY OF CHEMISTRY

ARTICLE TYPE

Cite this: DOI: 10.1039/xxxxxxxxxx

Growth of nanodroplets on a still microfiber under flow conditions†

Haitao Yu,[ab] Maaike Rump,[b] Shantanu Maheshwari,[b] Lei Bao,[a] and Xuehua Zhang[ca]*

Received Date
Accepted Date

DOI: 10.1039/xxxxxxxxxx

www.rsc.org/journalname

Surface droplets in microscale are of great interest for their relevance in broad droplet-based technologies. Deriving from the Ouzo effect, the solvent exchange process is a simple bottom-up approach to produce surface nano-/micro-droplets by the nucleation and growth mechanism. The oil oversaturation pulse is created as a good solvent (ethanol) for the oil displaced by a poor solvent (water) in the flow cell. In this work, we investigated the formation of surface droplets on an one-dimensional substrate (a single hydrophobic fiber with the diameter of 10 μm) in a flow. The droplet growth on the microfiber is enhanced as the fiber is perpendicular to the external flow direction, due to the coupled effects between the droplet formation and the local flow. On the other hand, droplets growth exhibits different growth dynamics as the fiber is placed parallel with the external flow direction. The general trend that surface droplets grow faster on fiber at higher flow rates is consistent with the situation on planar substrates. The coupled interactions between the growing droplets and the local flow conditions during solvent exchange process were further revealed in the simulations. The findings from this work will be valuable for design and utilization of the solvent exchange process to produce surface nanodroplets on microfiber under flow conditions and thus broaden the droplet-based application fields.

1 Introduction

Droplets hanging on fiber are often seen in nature, for example, morning dew on spider webs or rain drops on needle leaves of pine tree. This common phenomenon is important for many advanced technologies. In the method of single-drop microextraction, the drop on the fiber is in contact with the solution and extracts and separates the analyte for highly sensitive chemical analysis.[1,2] A nematic microdroplet on fibers can act as a microsensor to reveal the chirality of fibers.[3] Inspired by amazing symmetric patterns of water drops on spider webs, Jiang et al discovered importance of structural features of microfibers for droplet transport along the fiber and fabricated biomimic materials for water collection with exceptional performance.[4–6] Droplets on nanofibers exhibit fascinating wetting properties and self-propelled motion, which is desirable for enhanced heating transfer[4,7]. In an immiscible liquid medium, droplets on a fiber play an important role in filtration, microextraction, separation and sensing,[3,8–10] as well as in many oil-related applications where fibers are used as oil sorbents, coalescers, filters and separators.[8,11]

Intensive research interest has been drawn to understand the formation of droplets on microfibers during condensation. It is known that the droplet-on-fiber configuration includes two different geometries: an axisymmetric barrel shape or an asymmetric clam-shell shape. For uniform surface wettability and a constant fiber cross-sectional diameter, the clam-shell shape is preferred energetically when the droplet volume is small. The axisymmetric barrel shape will be more and more energetically favorable as the droplet becomes large enough.[12–14] According to classic heterogenous nucleation theory, droplets nucleate and grow on a substrate in an oversaturated environment. At the initial state when the size of droplets is very small, they grow as individual droplets on either one-dimensional (fiber) or two-dimensional (planar) substrates without confinement effect from

[a] Soft Matter & Interfaces Group, School of Engineering, RMIT University, Melbourne, VIC 3001, Australia.
[b] Physics of Fluids group, Department of Applied Physics, Mesa+ Institute, J. M. Burgers Centre for Fluid Dynamics & Max Planck Center Twente for Complex Fluid Dynamics, University of Twente, P.O. Box 217, 7500 AE Enschede, Netherlands.
[c] Department of Chemical and Materials Engineering, Faculty of Engineering, University of Alberta, Edmonton, Alberta T6G1H9, Canada.
* Corresponding Author, E-mail: xuehua.zhang@ualberta.ca

† Electronic Supplementary Information (ESI) available: Movies S1-6 are the droplets growth processes on the 10 μm fiber across the external flow direction, with different values of Pe and different fiber positions h_f during solvent exchange process. In data analysis process, time is defined as 0 when droplets start to form on fiber. See DOI: 10.1039/cXCP00000x/

‡ Additional footnotes to the title and authors can be included *e.g.* 'Present address:' or 'These authors contributed equally to this work' as above using the symbols: ‡, §, and ¶. Please place the appropriate symbol next to the author's name and include a `\footnotetext` entry in the the correct place in the list.

the substrates. As the droplets become larger, the growth dynamic of the droplets is related to the dimension of the substrate because of the difference in droplet coalescence. The time dependence of mean droplet diameter D follows the scaling law: $D \sim t^{\alpha}$, with a growth exponent $\alpha = 1/(D_d - D_s)$ [15,16]. Here D_d and D_s represent the dimension of surface droplet and substrate, respectively. The dimensions of substrate is defined as $D_d = 1$ for fibers and $D_d = 2$ for planar substrates, with the corresponding exponents $\alpha_{1D} = 1/2$ and $\alpha_{2D} = 1$.

A simple process for droplet formation at solid-liquid interfaces is solvent exchange where a solution of droplet liquid is displaced by a flow of a poor solvent. [17–19] A transient oversatuation of the droplet liquid is created at the mixing front, leading to the nucleation and growth of the droplets on channel walls. The size of droplets on the wall is determined by flow conditions, channel geometry, solution composition and surface properties. [17,20–23] The size of droplets on a homogenous substrate increases with the Peclet number of the flow with the power of $3/4$. [20,23] The duration of the droplet growth is related to the flow rate, $\sim Pe^{-1/2}$. The as-produced droplets are usually sub-femtoliter in volume, and less than 1 μm in height, therefore generally referred to as 'surface nanodroplets'.

What remains largely unexplored is nanodroplet formation on a fiber by the solvent exchange. Apart from the features of the droplet growth on the 1D dimension of the substrate, the new aspects are: how the droplet formation depends on the positioning and orientation of the fiber relevant to the flow, whether the formation the droplets from liquid-liquid phase separation at the mixing front influences the local flow transport, how stable the droplets are on the fibers in the flow. It is essential to address these aspects for controlled formation of nanodroplets on fibers by simple solvent exchange.

In this work, the nucleation and growth of oil droplets on a microfiber by the solvent exchange and the effects of nanodroplet formation on the local flow are experimentally and theoretically investigated. The diameter of the microfibers was 10 μm, placed in the flow channel at different locations. We observed strong dependence of droplet size on the fiber position. Meanwhile growing droplets on the microfiber increases the complexity of the local solution mixing. The coupled interactions between the growing droplets and the external flow are revealed by the simulations. The understanding of the nanodroplets on microfibers from this work can provide new opportunities for a range of technologies based on droplets, such as microextraction in chemical analysis and fabrication of beads-on-thread structures by using droplets as templates.

2 Experimental methods

2.1 Chemicals and hydrophobic microfiber

A stock solution was prepared by mixing the monomer (1,6-hexanediol diacrylate, HDODA) and an photo initiator (2-hydroxy-2-methylpropiophenone, HMPP) in a volume ratio of 10:1. Solution A was prepared by dissolving 2 mL stock solution into 100 mL of an 50 vol% ethanol aqueous solution. Solution B was water saturated with HDODA. The hydrophobic fiber used in the experiments was a glass fiber with a diameter of10 μm. The surface of the glass fiber was hydrophobilized with octadecyltrichlorosilane (OTS). To treat the surface, the glass fibers were first cleaned in piranha solution (70 vol% H_2SO_4: 30 vol% H_2O_2) at 75 $^{\circ}C$ for 30 mins. Then fibers were washed by water and fully dried at 120 $^{\circ}C$ for 2 hrs. It was important to minimize the exposure of OTS to water because moisture causes undesirable polymerization and large heterogeneity of the surface. In the next step, the cleaned and dried glass fibers were soaked in 0.5 vol% OTS in hexane solution in a sealed dry container for 4 hrs at room temperature. Finally, the OTS coated glass fibers were sonicated in the organic solvents, following the sequence of hexane, acetone, isopropanol (IPA) and ethanol for 15 mins each. All chemicals used in the experiments were purchased from Sigma-Aldrich.

Table 1 Flow conditions and positions of the microfiber during the solvent exchange. Here Q is the flow rate, Pe is the Peclet number, Re is the Reynolds number, h_f is the fiber position in the channel, and h_c, the channel height.

No.	$Q\ (\mu L/min)$	Pe	Re	$h_f\ (mm)$	$h_c\ (mm)$	h_f/h_c
1	50	55.5	0.02	1.3	2.6	0.5
2	100	111	0.04	1.3	2.6	0.5
3	200	222	0.08	1.3	2.6	0.5
4	400	444	0.17	1.3	2.6	0.5
5	50	111	0.04	0.65	2.6	0.25
6	50	111	0.04	1.95	2.6	0.75

2.2 Droplet formation by solvent exchange

A schematic drawing of the experimental setup is shown in Fig. 1a. The hydrophobic microfiber was placed inside a fluid chamber with a distance of h_f from the bottom wall. In a top-view sketch (Fig. 1b), the microfiber is across (perpendicularly to) the external flow direction from left to right shown as the blue arrow. The total height of the chamber h_c was 2.6 mm, the width was 15 mm and the length was 50 mm in all experiments. To investigate the situation of droplet growth from position effect, the fiber position h_f was shifted to different heights with $h_f/h_c = 0.25$ and $h_f/h_c = 0.75$. As comparison, the orientation of fiber was also rotated 90° to be parallel to the flow direction.

During the solvent exchange process, the flow cell was first filled with solution A and then exchanged by a flow solution B. The flow rate was controlled by the syringe pump. The Peclet number of $Pe = Uh/D_c$ and Reynolds number $Re = Uh/\nu$ are used to show the external flow condition. Here, D_c means the diffusivity ($D_c \approx 1.0 \times 10^{-9}\ m^2/s$) and ν is the viscosity ($\nu = 10^{-6} m^2/s$). [24,25] All the external flow conditions in this work are in the laminar region ($Re < 1$) as listed in Table 1.

2.3 Imaging analysis of growing droplets

The process of the droplet growth was recorded with a camera through a reflection mode optical microscopy (Huvitz HRM-300). The mean diameter D of droplets on fiber over time was extracted from the experimental results by Matlab software, following the process in Fig. 2a. First, all droplets on the left side of fiber were identified. Then, we did the circle fit through each de-

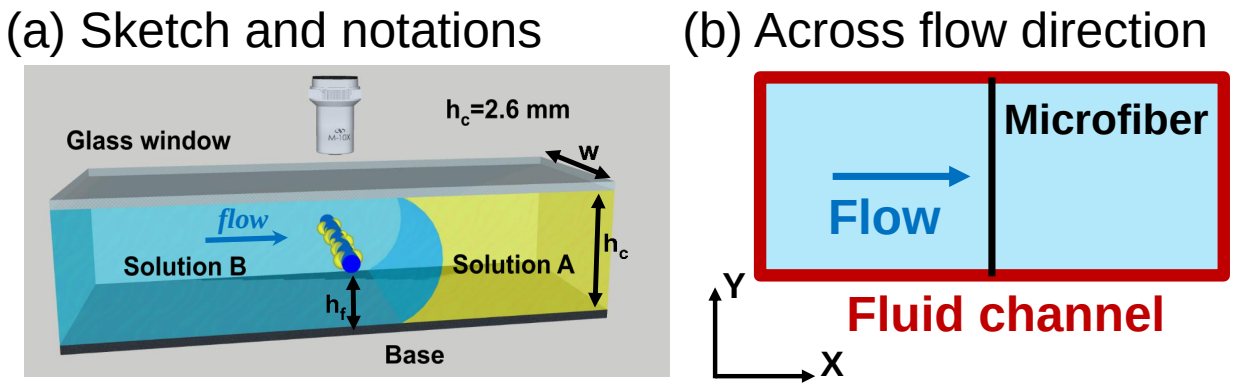

Fig. 1 (*a*) Schematic drawing of the solvent exchange process to produce surface droplets on a hydrophobilized fiber. The droplets were observed through the top glass window. h_c and h_f are the height of channel and fiber, respectively. $h_c = 2.6mm$. w is the width of the channel. (*b*) A top-view sketch of the experimental setup with an external flow direction from left to right. The glass fiber is placed perpendicular to the flow direction.

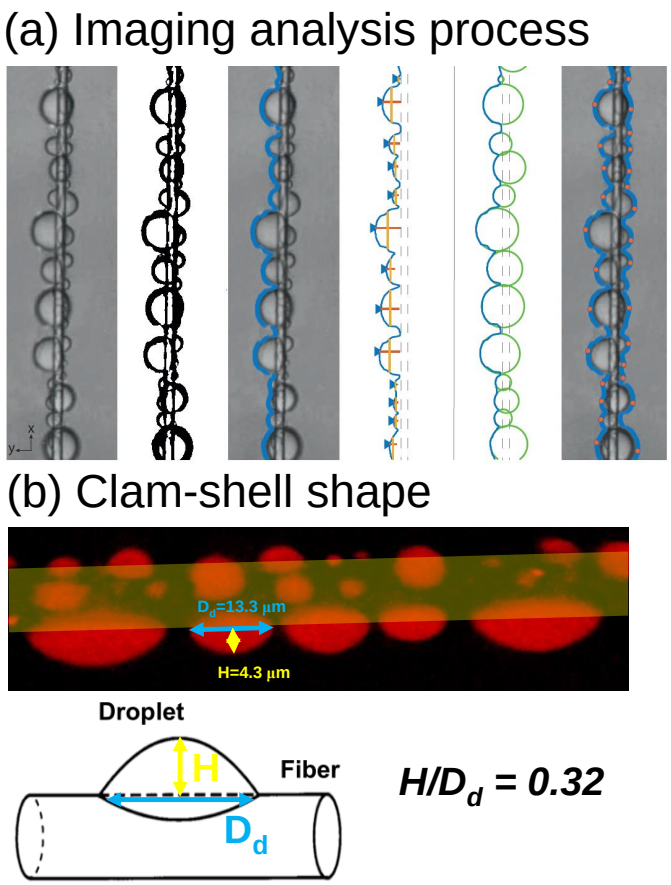

Fig. 2 (*a*)Imaging analysis process by using Matlab software: 1. Image contrast enhancement and binarization; 2. Edge detection; 3. Surface droplets detection; 4. Circle fit through all detected droplets. The mean diameter of droplets was obtained as the intersection points between the fitted circles and the surface of the fiber. (*b*)Confocal microscopic image of surface droplets on microfiber. The shape of the droplets (dyed in red) is a clam shell. The definitions of the lateral diameter D_d and the height H is notated in the sketch. The ratio of H to D_d is about 0.32.

tected droplet and the diameter of each droplet which was defined as the distance between the intersections of the fitted circle and the microfiber. The same procedures were further repeated for the droplets on the right side of the fiber and thus obtained the mean diameter as the intersection points between the fitted circles and the surface of the fiber. The analysis program completes these procedure for every frame. Unfortunately, there are two main issues existing during analysis process. First, the clouds of surrounding oil droplets in flow, especially the clouds in a layer shape at small *Pe* severely shielded the process of droplets growth on microfiber. Second, we can not record the droplet growth on microfiber until the final state because the homogeneous nucleation and growth of droplets in bulk above the microfiber location would dramatically reduce the light quantity in the latter part of the solvent exchange process.

2.4 Characterization of droplet morphology

At the end of solvent exchange, surface nanodroplets on microfiber were polymerized under a UV lamp (365nm, 20W) for 15 mins. The geometry of droplets on microfiber was characterized by a confocal microscopy. A representative three-dimensional image is demonstrated in Fig. 2b, illustrating the droplets on microfiber is in a clam-shell shape.[12,14] According to one representative droplet on fiber with the lateral diameter D_d of 13.3 μm and the height H of 4.3 μm, the ratio of H to D_d was calculated to equal 0.32.

2.5 Comsol simulations

Simulations were performed to reveal the flow around the fiber by using Comsol Multiphysics (COMSOL AB, Stockholm, Sweden), following the protocol reported in ref.[23]. For the flow with *Pe* and *Re* same as those in the experiments, the velocity profile was calculated by solving the Navier-Stokes equation with no-slip boundary condition at the fiber surface, but a slip boundary at the surface of oil droplets. The oil concentration field with space & time was solved based on the time dependent diffusion equation, coupled with velocity profile.

3 Results and discussion

3.1 Nucleation and growth of droplets on the microfiber

Representative snapshots of droplet growth on the fiber perpendicular to the flow direction with $Pe = 444$ and $Re = 0.16$ are illustrated in Fig. 3a. Oil nanodroplets nucleated and grew on microfiber with a diameter of 10 μm in flow during solvent exchange. At time ~ 0 s, the droplets start to form on the fiber. At 50 s, the diameters of surface nanodroplets on the fiber reached dozens of micrometers and still kept growing. Following the imaging analysis process, the mean diameter D and the number density of nanodroplets on the microfiber were plotted as function of time in Fig. 3b,c. The number of nanodroplets on the microfiber of unit length (mm) is in a bell shape, increasing to about 50 droplets in 10 s and then decreasing. The decrease in the number density is due to the coalescence of surface droplets. The mean diameter D increases to about 40 μm in 40 s. (We note that all D in this work refers to the mean diameter of droplets.) The peak of the number density occurs when D is comparable the diameter of microfiber (10 μm) at 10 s.

More representative snapshots of droplet growth process at different Pe numbers are demonstrated in Fig. 4a,b. The rate of the droplet growth is slower at smaller Pe. For example, at about 30 s, the size of droplets on microfiber at $Pe = 444$ is larger than that at $Pe = 111$ and $Pe = 55.5$. Based on the quantitative analysis, the mean diameter D of droplets is plotted as a function of time for different Pe in Fig. 5a. The slope from a linear fitting of the data is used to characterise droplet growth rate μ_d. Fig. 5b shows that the droplet growth rate μ_d is faster at larger Pe. The slope increases by more than one magnitude with the increase in Pe from 55.5 to 444. At the later stage of the solvent exchange, we observed the droplets coalesced rapidly and were very mobile on the fiber. By the end, only a few large droplets remain on the fiber.

The faster growth rate of the droplets at higher Peclet number is consistent with the effect of flow conditions on the growth dynamics of nanodroplets during the solvent exchange. Our previous work on planar substrates showed that the final droplet volume scales with $Pe^{3/4}$, assuming a constant contact angle growth mode of droplets with a shape of spherical cap.[19] Here we cannot obtain an exact form of the temporal evolution in the droplet volume, due to the complicated shape of the droplets on fiber. However, the general trend that droplets grow faster at higher flow rates is consistent with the situation on planar substrates.

As the mirofiber was placed parallel to the flow direction as sketched in Fig. 6a, no clusters of droplets form along the fiber in the flow, suggesting that the influence from the microfiber on the local flow was reduced. Based the optical images demonstrated in Fig. 6b, the diameters of the final oil droplets formed on microfiber is on microscale. The trend of larger drolepts at larger Pe is also indicated. Specifically, when $Pe = 444$ in this parallel set, D of the final droplets on microfiber was 13.9 μm. With quantitative analysis of D drawn in a double logarithm plot (Fig. 6c) as a function of Pe, a linear fitting with the slope of $1/4$ (purple dashed line) was obtained, which represents the scaling law: $D \sim Pe^{1/4}$, in a good agreement with our theoretical understanding of droplet formation in diffusive growth mode on the substrate in ref.[20]. This suggests it is feasible to control the surface droplets formation on the microfiber in flow by mediating flow conditions.

There is significant difference in the growth dynamics of droplets on the fibers in two orientations. Droplets on the fiber along the flow direction were much smaller than those on the fiber across the flow. Such significant difference suggests that a coupled effect from the droplet formation and the local flow, occurring when the fiber is placed against flow direction. This coupled effect will be further demonstrated by dynamics of droplets in the flow (not attached to the fiber) as below.

3.2 Dynamics of droplets near the fiber

As shown in Fig. 4(a), at the initial stage at time of 0 s small droplets suspended in the solution moved along the flow direction, creating a uniform cloudy background. With the time, more droplets stay in a zone ahead of the fiber. The droplet zone ahead of the fiber was discrete at 5 s, and became a continuous stripe after 3 s. The thickness of the zone slightly increased by the time of 11 s. Interestingly, during the period of building up the front droplet zone, there is also a visible depleted zone adjacent to the droplet zone, further away from the fiber. The presence of the depletion zone suggests that development of the interfacial droplet excludes the droplets carried by the flow.

The droplet zone in the solution was dramatically interrupted at time of 20 s, accompanying with visible growth of the droplets on the fiber. A part of the droplet cluster started to move, swirling around the fiber and spreading downward. The clusters eventually smeared out and eventually vanished in the flow. At those locations touched by the swirling droplets, those still droplets on the fiber became immediately larger, possibly due to enhanced droplet coalescence. As the droplet cluster cleared off from the zone near the fiber at 40 s, the clear depletion zone still remained ahead of the fiber, clearly suggesting that the droplet formation on the fiber excluded the droplets from the flow, same effects observed at the earlier time from 5 to 11 s when the interfacial droplet zone was building up. The above evolution of the droplet clouds can be divided into two stages. At stage I, droplets gradually accumulate in the zone next to the fiber. At stage II, droplet clouds move and detach from the zone.

It is noticeable that both the duration of stage I and the maximal thickness of the droplet zone by the end of stage I are related to the flow rate. Fig. 7(a) shows the droplet zone by the end of stage I at different Pe. The maximal thickness of the zone was larger at lower Pe, attributed to enhanced mass transfer or shorter time for cumulative effect in a faster flow. Based on quantitative analysis, we plotted the duration of stage I as a function of $1/\sqrt{Pe}$ (Fig. 7b). The red dashed lines illustrate the linear relationship of stage I duration versus $Pe^{-1/2}$.

Both the droplet motion and additional tracing microparticles in flow show that presence of the fiber itself did not introduce asymetric flow field around it, similar to the symmetric streamline formed when a simple flow cross a fiber in a laminar flow. However, when droplets formed on the fiber, the symmetric sim-

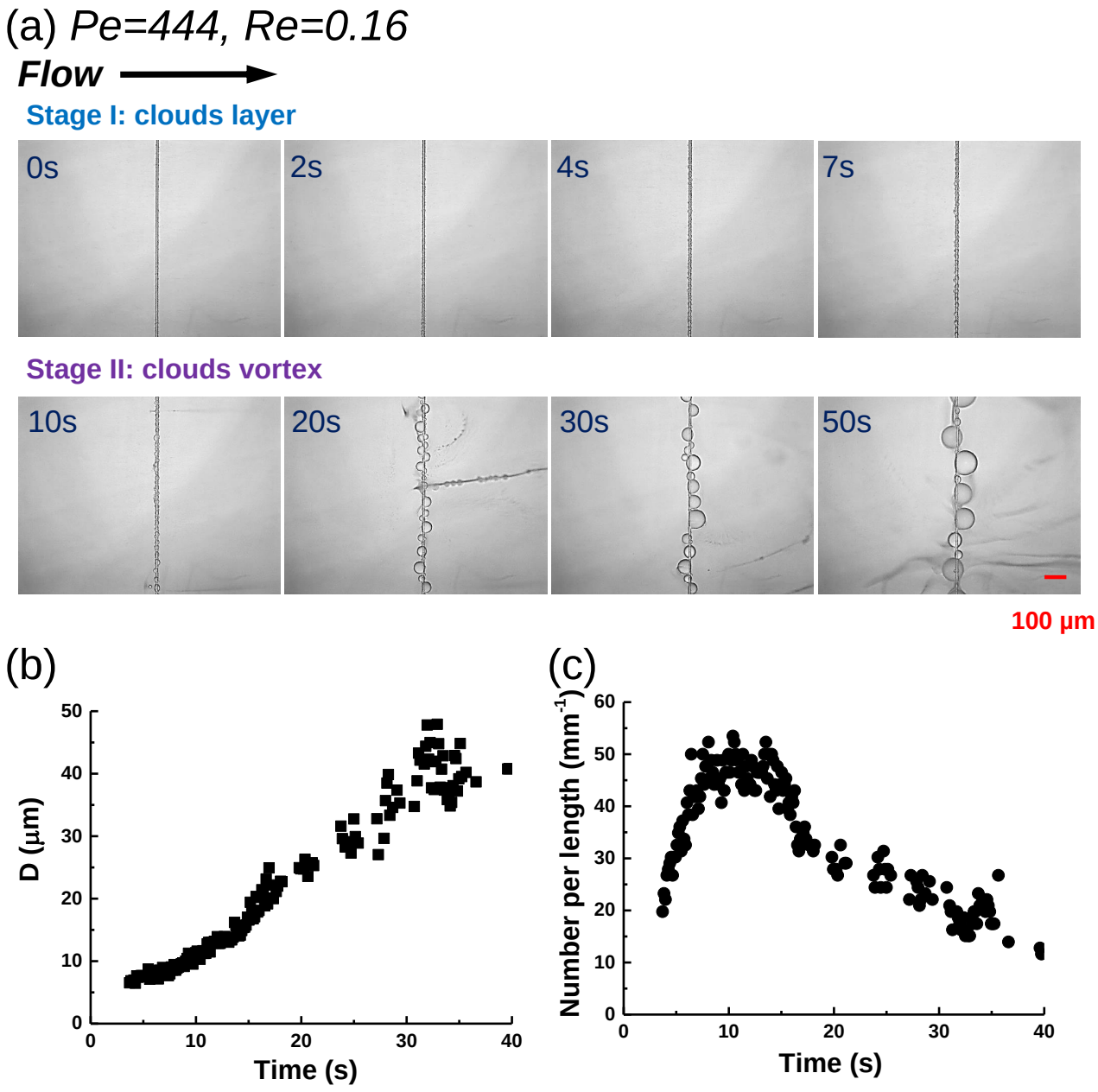

Fig. 3 Dynamical process of droplet growth on the microfiber in the flow with $Pe = 444$, $Re = 0.16$, and $h_f/h_c = 0.5$. The onset of the droplet formation was set as $t_0 = 0\ s$. (*a*)Time course snapshots of the droplets on 10 μm fiber in flow. The direction of the flow was from left to right, indicated by the black arrow. The entire process is divided into two stages according to the morphology of surrounding clouds of tiny oil droplets in flow: stage I: clouds layer; stage II: clouds vortex. Length of the scale bar: 100 μm. (*b*) the mean diameter D and (*c*) the number of surface droplets on microfiber of unit length (millimeter) are plotted as a function of time. We note that all D in this work refers to the mean diameter of droplets.

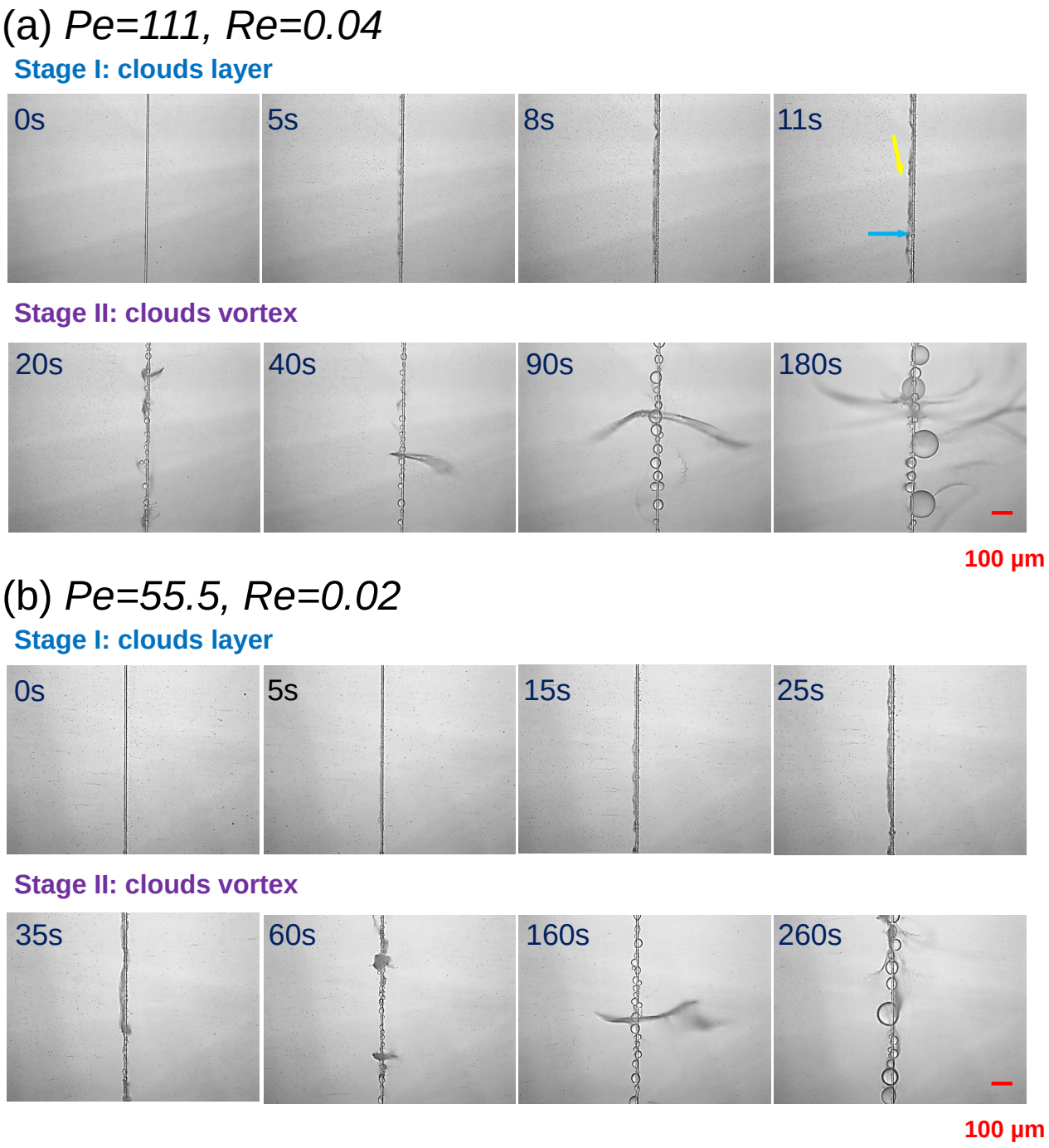

Fig. 4 Snapshots of the surface droplets growth process on microfiber in flow with (*a*) $Pe = 111$ and (*b*) $Pe = 55.5$ at a constant position $h_f/h_c = 0.5$. The blue and yellow arrows point out the front droplet zone and depletion zone, respectively. Scale bar: 100 μm.

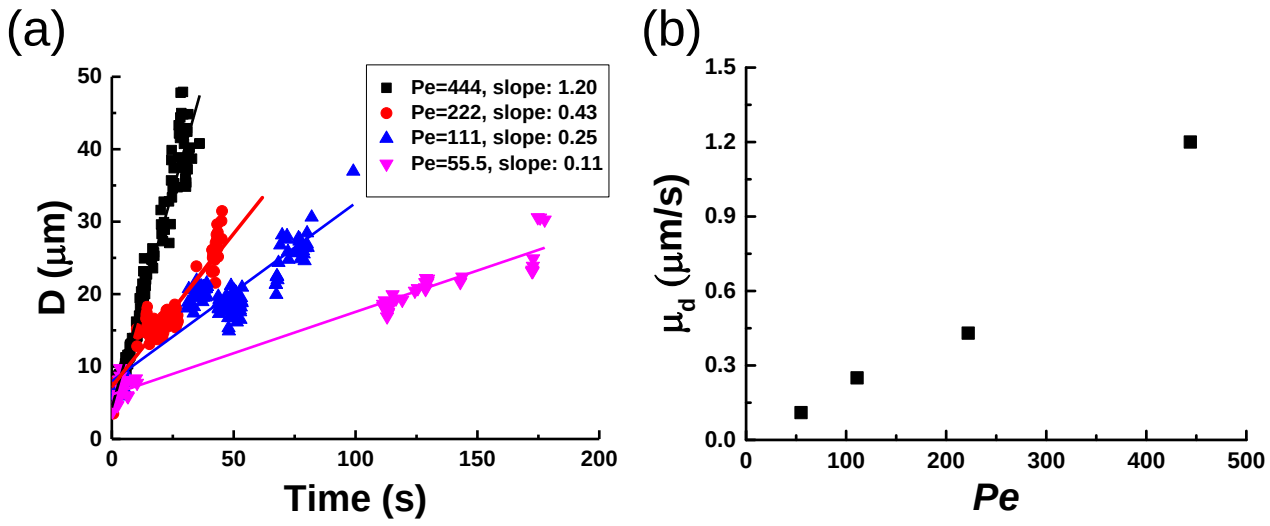

Fig. 5 (*a*) The plot of droplet mean diameters D verses time at different Pe values: 55.5, 111, 222, and 444. As the clouds was more obvious at smaller Pe, the analysis of droplet growth process was severely influenced by the surrounding clouds and thus missed many data points. Meanwhile, in the late stage of clouds vortex, the view was totally shielded by the formation of bulk droplets above the focus position. The droplet growth processes have been simplified by using a linear fitting to illustrate the growth trend. (*b*) The growth rates of D (slopes in (*a*), μ_d) as a function of Pe.

ple flow field could no longer be possible. The process of phase separation for droplet formation may lead to dramatic change of the local solution composition and magnify the difference in the concentration gradient between the front and the back for the fiber.

This local concentration gradient is also responsible for the phenomenon that the droplet in the flow are excluded by the droplet cluster. During solvent exchange process, solution A was 50% ethanol aqueous solution and solution B was water. The concentration field was uniform at the mixing front without any perturbation. The droplets transport by the external flow, smoothly passing the fiber before the nucleation of droplets on the fiber. However, the concentration gradient became highly heterogeneous spatially, as the local composition was alternated by the phase separation for the droplet formation on the fiber. It is not rare that chemical potential from the phase separation drives mechanical motion, such as in self-propelled droplets in partially miscible solvent and splitting droplets and dancing droplets.[26–29] The exclusion of the droplets from the zone may be also related to an interesting colloidal behaviour in the mixture with a concentration gradient, called diffusiophoresis.[30–32] The chemical energy of concentration gradients is converted into the mechanical energy for the motion of the colloids. Our latest work also showed that the concentration gradient from phase separation drove fast motion of microparticles in a diffusive field.[33] The motions of the tiny droplets in bulk fluid driven by the diffusiophoresis are against the external flow direction, as illustrated in Fig. 8a. Occasionally we also observed that some droplets within the zone were ejected out, also in the direction against the flow. As solvent exchange proceeds, the concentration gradient became less. The shear from external flow eventually took over the effect from chemical heterogeneity, so the droplet clusters were washed off from the fiber.

These results have suggested that local mixing of the flow has been dramatically enhanced when droplets formed on the fiber against flow direction. Such flow condition coupled with the growing droplets leads to the accelerated growth of droplets on the fiber. As the fiber was placed along the flow direction, even the droplets formed on the fiber, the local flow profile remained symmetric. Therefore,there is no droplet cluster formed in the flow and the droplet growth on the fiber is more moderate.

3.3 Different fiber position h_f/h_c

In the following, we will focus on the droplet formed on the fiber against flow direction and located at different posisions. The optical images in Fig. 9 show the droplet formation on the microfiber located at different locations along the Z axis of the channel with the values of h_f/h_c to be 1/4, 1/2, and 3/4 in the experiments. The external flow rate was same at $Pe = 111$, $Re = 0.04$ and channel height $h_c = 2.6\ mm$. At the transition from stage I to stage II, there is significant difference in the position and thickness of the droplet zone. Little amount of droplets accumulated at the *left* side of the microfiber at $h_f = 1/4h_c$, in contrast to a thick layer of droplet zone at the *left* side of the microfiber when $h_f = 1/2h_c$. Remarkably, the droplet zone switched to the *right* side of the microfiber at $h_f = 3/4h_c$. It is interesting why the thickness of the droplet zone and even the position relevant to the fiber in flow direction changes with the position of fiber.

To understand these experimental results, we will discuss the influences from two aspects during solvent exchange process: gravitational effect and buoyancy effect. Specifically, gravitational effect plays an important role on the velocity field, reported in ref.[21]. With $h_c = 2.6\ mm$, the crucial control parameter (Archimedes number Ar) equals $17224 >> 1$, which means the maximum velocity position is very close to the bottom wall. So the local flow velocity decreases as the microfiber position is shifted upwards and thus the local Pe_{h_f/h_c} decreases as well: $Pe_{1/4} > Pe_{1/2} > Pe_{3/4}$. As we explained before, the clouds layer

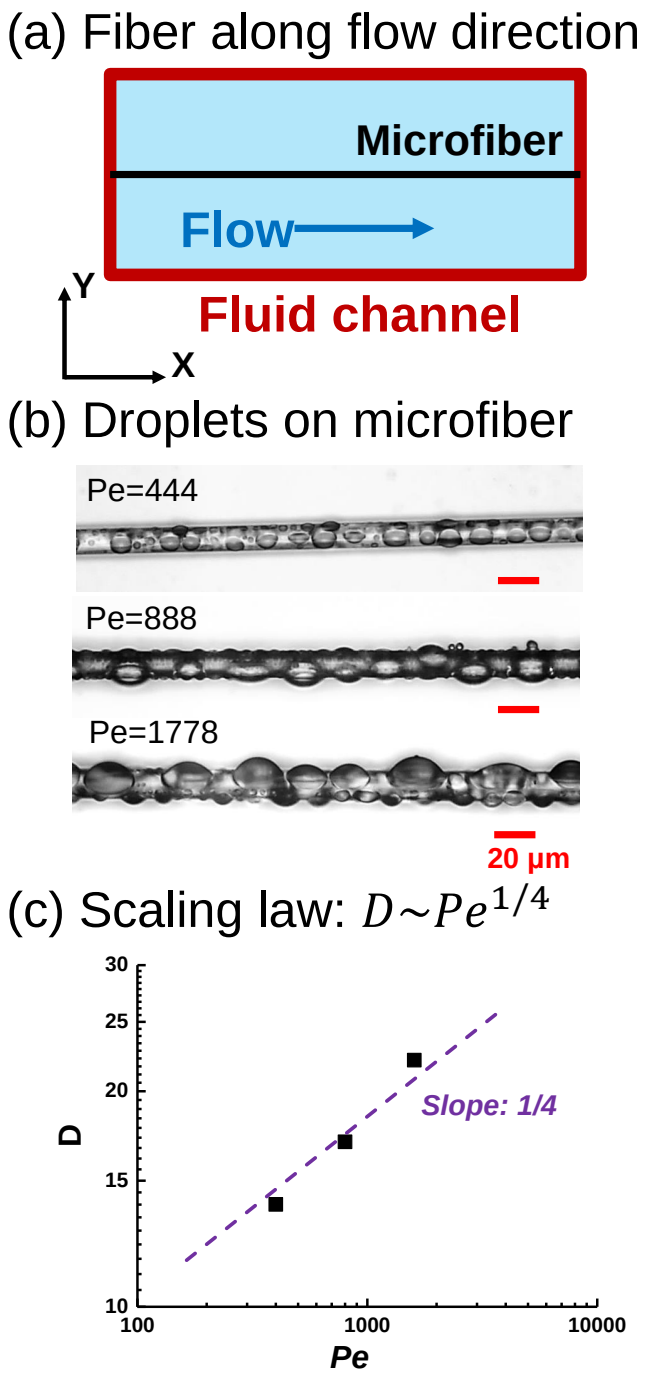

Fig. 6 Droplet growth on the OTS-glass microfiber that was parallel with the external flow direction.(*a*) A top-view sketch of experimental set with the microfiber parallel with the external flow direction, from left to right. (*b*) Optical images of droplets formation on microfiber at different Pe values of solvent exchange process: 444, 888, and 1778. Scale bar: 20 μm. (*c*) Mean diameters D of droplets formed on microfiber versus Pe in a double-logarithm plot. Purple dashed line represents the linear fitting with a slope of 1/4, which represents the scaling law: $D \sim Pe^{1/4}$.

will be thicker at smaller Pe. On the other hand, the density difference between two solutions used in solvent exchange process will lead to the buoyancy-driven convection roll in the fluid channel, representing by the estimated value of Rayleigh number, 5.7×10^5 (much larger than the critical Rayleigh number, 1708) when $h_c = 2.6\ mm$.[20]

In the experiments, we exactly observed that the droplets in the solution were flowing from right to left at $h_f = 3/4h_c$, marked as the arrow in Fig. 9c, which was against the direction of the external flow from left to right. This reverse flow direction at high position with large h_f/h_c value was induced by the buoyancy-driven convection roll in the flow cell, dominated by a large value of Rayleigh number. Correspondingly, under the right-to-left flow direction, the clouds layer at $h_f = 3/4h_c$ reasonably appeared at the right side of the fiber. Overall, all these experimental results show the formation and motion of clouds in flow closely couple with the local flow condition.

3.4 Comsol simulation

We simulate the droplet formation on fiber in a flow with the Comsol simulations. As an oil oversaturation was sent in flow, oil oversaturation pulse is clearly affected when one microfiber (marked as circle 1) exists as shown in Fig. 10a. Specifically, when there is only a microfiber in the channel, the oil oversaturation profiles above and below the microfiber are symmetric. However, if there is a surface droplet (marked as circle 2 in Fig. 10b) with a diameter of 10 μm on microfiber (the droplet diameter D_2 equals to the fiber diameter D_1, which means $D_2/D_1 = 1$), the asymmetry of oil oversaturation profile is revealed by the simulations, deriving from the asymmetrical geometry of oil droplet on microfiber. As the droplet grows, for example, $D_2/D_1 = 3$, the asymmetric geometry of droplet on microfiber develops and thus contributes more to the corresponding asymmetry of the oil oversaturation profile. These would work as the perturbation to the flow and further result in the clouds vortex. Meanwhile, it is worthy to mention that, besides the asymmetry simulated on X-Y plant in Fig. 10, the asymmetry of droplets on fiber also exists on other planes (X-Z plane, and Y-Z plane). All these contribute to the dynamical behaviour of the droplet cluster. In the actual solvent exchange process, the situation of concentration gradient may be much more complicated. The real concentration gradient may be also influenced by mixing of multiple components in the flow, phase separation of droplets and collective interactions among droplets. More comprehensive simulation technique will be required to take all these factors into consideration.

4 Conclusion

In summary, a hydrophobic microfiber with a diameter of 10 μm was located in flow as the substrate for surface oil droplets formation by solvent exchange process. When the microfiber was across the external flow direction, the droplet growth on microfiber was dramatically enhanced due to the coupled effects from the droplet formation and the local flow. These coupled effects were clearly revealed by the dynamics of droplets in the flow. Different growth dynamics was observed for droplets on the microfiber as the fiber

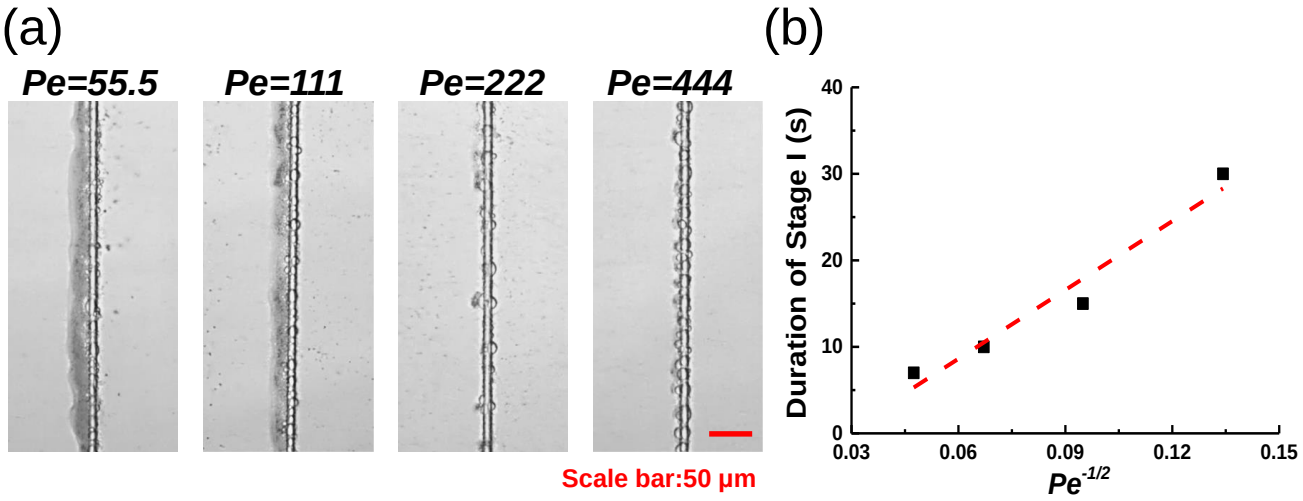

Fig. 7 The droplet zones by the end of stage I at different values of Pe and constant fiber position $h_f/h_c = 0.5$. (*a*) The snapshots of the droplet zones with the maximum thickness under different external Pe values of 55.5, 111, 222 and 444. Scale bar is 50 μm. (*b*) The plot of the duration of Stage I (the clouds layer stage) as a function of Pe number during solvent exchange process.

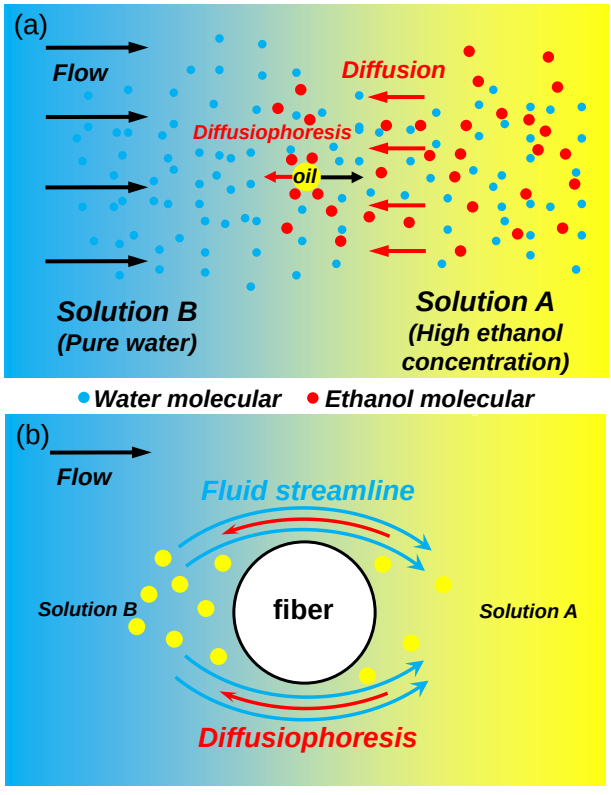

Fig. 8 Schematic diagrams of diffusiophoresis during solvent exchange process at (*a*) diffusive domination and (*b*) diffusive-advective domination surrounding the microfiber.

orientation was rotated to along the external flow direction. The general trend that surface droplets grow faster on fiber at higher flow rates is consistent with the situation on planar substrates. Moreover, the asymmetry of oil oversaturation pulses deriving from the asymmetric geometry of surface droplets on microfiber was revealed by the Comsol simulations, which demonstrated the coupled interactions between the growing droplets and the local flow conditions. This finding will guide the controlled formation of surface nanodroplets on the microfiber during solvent exchange process and provide a droplet-based platform for the application of surface nanodroplets in flow.

5 Acknowledges

H.Yu acknowledges the Vice Chancellor PhD Scholarship in RMIT University. L.B acknowledges the support from RMIT Vice Chancellor Postdoctoral Fellowship and Australian Research Council (ARC, LP140100594). X.H.Z. acknowledges support from Australian Research Council through the schemes of Future Fellowship (FT120100473) and Linkage Project (LP140100594), and the support from Future Energy Systems, University of Alberta. We also acknowledge technical support from the RMIT Micro-Nano Research Facility.

References

1 S. Uemura, M. Stjernström, J. Sjödahl and J. Roeraade, *Langmuir*, 2006, **22**, 10272–10276.
2 M. A. Jeannot and F. F. Cantwell, *Analytical Chemistry*, 1996, **68**, 2236–2240.
3 L. E. Aguirre, A. D. Oliveira, P. L. Almeida, M. Ravnik, S. Copar and M. H. Godinho, 2015, 1–6.
4 Y. Zheng, H. Bai, Z. Huang, X. Tian, F. Q. Nie, Y. Zhao, J. Zhai and L. Jiang, *Nature*, 2010, **463**, 640–643.
5 X. Tian, Y. Chen, Y. Zheng, H. Bai and L. Jiang, *Advanced Materials*, 2011, **23**, 5486–5491.
6 H. Bai, J. Ju, Y. Zheng and L. Jiang, *Advanced Materials*, 2012, **24**, 2786–2791.

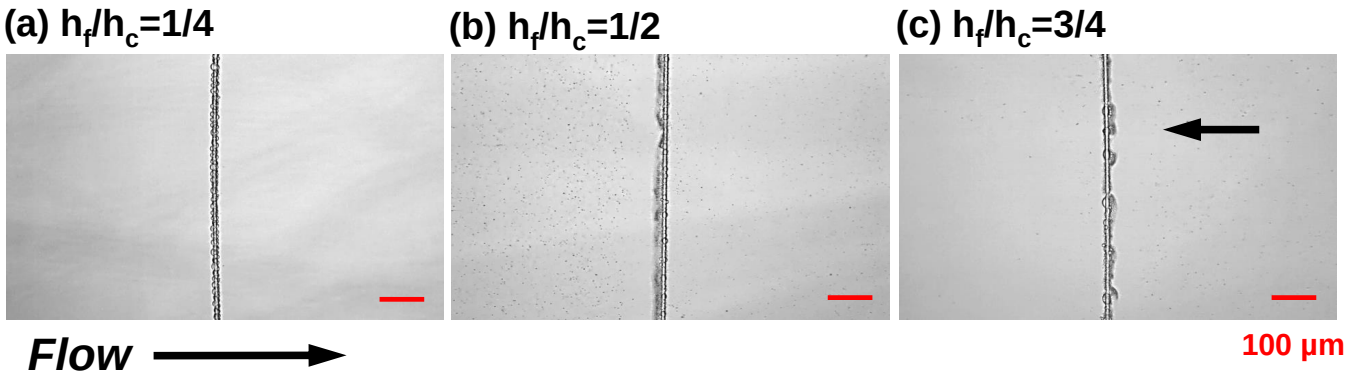

Fig. 9 Optical images of the transaction from clouds layer into clouds vortex surrounding the microfiber at different positions (*a*) $h_f/h_c = 1/4$, (*b*) $h_f/h_c = 1/2$, and (*c*) $h_f/h_c = 3/4$. The heights of channel $h_c = 2.6mm$, $Pe = 111$, $Re = 0.04$ are constant. Scaling bar: 100 μm. The external flow direction is from left to right. Black arrow in (*c*) shows the local flow direction is from right to left.

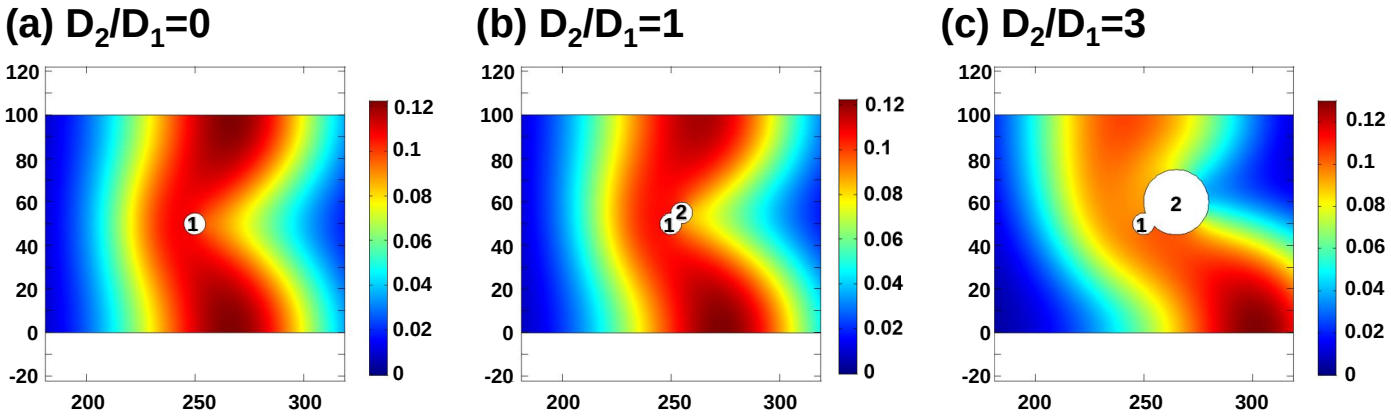

Fig. 10 Comsol simulations for the profiles of oil oversaturation pulse at different situations with the values of D_2/D_1: (*a*) 0, (*b*) 1, and (*c*) 3, respectively. Circle 1 means the hydrophobic glass fiber with a diameter D_1 of 10 μm and Circle 2 means the oil drop grown on the fiber with the diameters D_2: 0, 10, and 30 μm, respectively. X axis and Y axis in plots show the position of the channel in the X-Z plane in the simulation in the unit of μm. The scale bars in color represent oil oversaturation with a unit of mol/L. $Pe = 444$ and $Re = 0.17$ in this simulation.

7 C. Dawson, J. F. Vincent, G. Jeronimidis, G. Rice and P. Forshaw, *Journal of Theoretical Biology*, 1999, **199**, 291 – 295.

8 A. Méndez-Vilas, A. B. Jódar-Reyes and M. L. González-Martín, *Small*, 2009, **5**, 1366–1390.

9 C. Duprat, S. Protière, A. Y. Beebe and H. A. Stone, *Nature*, 2012, **482**, 510–513.

10 O. Arjmandi-Tash, N. M. Kovalchuk, A. Trybala, I. V. Kuchin and V. Starov, *Langmuir*, 2017, acs.langmuir.6b04094.

11 O. Carmody, R. Frost, Y. Xi and S. Kokot, *Surface Science*, 2007, **601**, 2066–2076.

12 G. McHale and M. Newton, *Colloids Surf., A*, 2002, **206**, 79–86.

13 M. Mei and D. Shou, *Soft Matter*, 2013, 10324–10334.

14 H. B. Eral, D. J. C. M. 'T Mannetje and J. M. Oh, *Colloid and Polymer Science*, 2013, **291**, 247–260.

15 D. Fritter, C. M. Knobler and D. A. Beysens, *Physical Review A*, 1991, **43**, 2858–2870.

16 D. Beysens, *C. R. Phys.*, 2006, **7**, 1082–1100.

17 D. Lohse and X. Zhang, *Rev. Mod. Phys.*, 2015, **87**, 981–1035.

18 X. H. Zhang and W. Ducker, *Langmuir*, 2008, **24**, 110–115.

19 J. Zhang, E. Luijten and S. Granick, *Annu. Rev. Phys. Chem.*, 2015, **66**, 581–600.

20 X. Zhang, Z. Lu, H. Tan, L. Bao, Y. He, C. Sun and D. Lohse, *Proceedings of the National Academy of Sciences*, 2015, **112**, 9253–9257.

21 H. Yu, Z. Lu, D. Lohse and X. Zhang, *Langmuir*, 2015, **31**, 12628–12634.

22 Z. Lu, S. Peng and X. Zhang, *Langmuir*, 2016, **32**, 1700–1706.

23 H. Yu, S. Maheshwari, J. Y. Zhu, D. Lohse and X. Zhang, *Lab Chip*, 2017, **17**, 1496–1504.

24 B. R. Hammond and R. H. Stokes, *Trans. Faraday Soc.*, 1953, **49**, 890–895.

25 E. E. Hills, M. H. Abraham, A. Hersey and C. D. Bevan, *Fluid Phase Equilib.*, 2011, **303**, 45–55.

26 C. Jin, C. Krüger and C. C. Maass, *Proceedings of the National Academy of Sciences*, 2016, **114**, 5089–5094.

27 C. Kruger, G. Klos, C. Bahr and C. C. Maass, *Physical Review Letters*, 2016, **117**, 1–5.

28 B. Liebchen, D. Marenduzzo, I. Pagonabarraga and M. E. Cates, *Physical Review Letters*, 2015, **115**, 1–5.

29 I. Buttinoni, J. Bialké, F. Kümmel, H. Löwen, C. Bechinger and T. Speck, *Physical Review Letters*, 2013, **110**, 1–5.

30 D. Velegol, A. Garg, R. Guha, A. Kar and M. Kumar, *Soft Matter*, 2016, **12**, 4686–4703.

31 A. S. Khair, *Journal of Fluid Mechanics*, 2013, **731**, 64–94.

32 P. O. Staffeld and J. A. Quinn, *Journal of Colloid And Interface Science*, 1989, **130**, 69–87.

33 Z. Lu, M. H. K. Schaarsberg, X. Zhu, L. Y. Yeo, D. Lohse and X. Zhang, *Proceedings of the National Academy of Sciences*, 2017, **114**, 10332 LP – 10337.

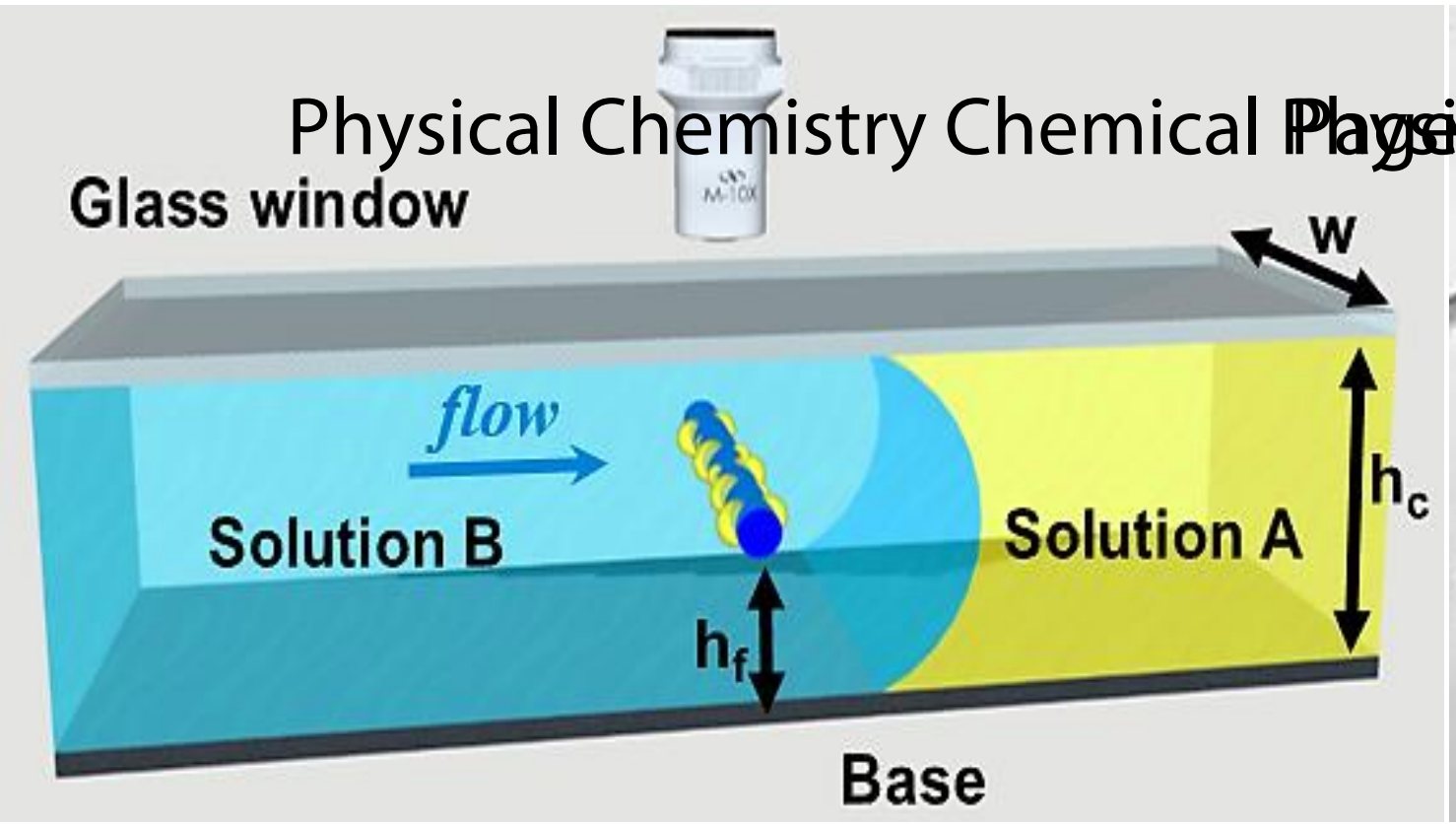

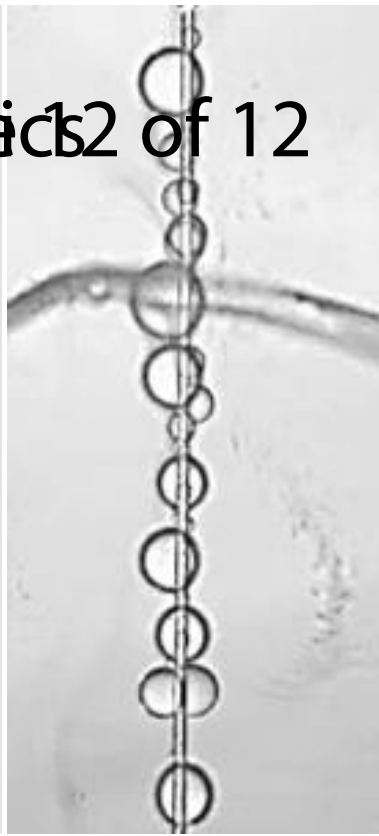

The couple effects from the droplet formation and the local flow dramatically enhanced the droplet growth on microfiber in flow.